IEEE Access
Multidisciplinary | Rapid Review | Open Access Journal

Received November 2, 2021, accepted December 2, 2021, date of publication December 7, 2021,
date of current version December 30, 2021.

Digital Object Identifier 10.1109/ACCESS.2021.3133663

A Novel Four-Arm Planar Spiral Antenna for GNSS Application

LILI GUO[1,2], PEIHUA ZHANG[2,3], FANCHAO ZENG[4], ZHIYA ZHANG[1], AND CHENGBIN ZHANG[1]

[1]National Key Laboratory of Science and Technology on Antennas and Microwaves, Xidian University, Xi'an 710071, China
[2]Shaanxi Key Laboratory of Integrated and Intelligent Navigation, Xi'an 710068, China
[3]The 20th Research Institute of China Electronics Technology Corporation, Xi'an 710068, China
[4]University of Technology Sydney, Sydney, NSW 2007, Australia

Corresponding authors: Zhiya Zhang (zyzhang@xidian.edu.cn) and Fanchao Zeng (zengfc123@163.com)

This work was supported by the Foundation of Shaanxi Key Laboratory of Integrated and Intelligent Navigation under Grant SKLIIN-20190101.

ABSTRACT This letter introduces a novel four-arm planar spiral antenna which provides a perfect circular polarization radiation for Global Navigation Satellite System applications. The antenna mainly consists of four parts: an Archimedes spiral radiation area, an impedance matching area composed of an appropriately sized metal coupling disc and quasi-coaxial structures, a wideband four-output-ports feed network with equal magnitude and consistent 90° phase shift, and a set of chokes with unequal height. The metal coupling disc and quasi-coaxial structures are used as an impedance transformer to provide broadband matching between the 50Ω input impedance and the high impedance of the radiation area. The novel choke can ensure the radiation characteristics and stable phase center of the antenna in broadband range. Based on these designs, the proposed four-arm planar spiral antenna shows the impedance bandwidth (VSWR $<$ 1.5) and 3-dB axial ratio bandwidth of 1.1-1.7GHz, and simultaneously realizes radiation gain greater than 7.4 dBic and phase center deviation (PCD) less than 1.5mm.

INDEX TERMS Broadband, four-arm spiral antenna, GNSS application, novel choke, stable phase center.

I. INTRODUCTION

In satellite navigation communications, the performance of the antenna determines the stability of the system. Circular polarization (CP) antennas have been widely used due to their advantages in reducing interference and polarization mismatch. At present, many single-band, dual-band and triple-band CP antennas are used in the Global Navigation Satellite System (GNSS). In order to consider the influence of design cost and mutual coupling, broadband circularly polarized antennas that can cover the whole frequency band (1.164-1.612GHz) of GNSS have gradually become a trend [1], [2].

Spiral antennas get increasingly attentions for their good characteristics of broadband and circular polarization. Most of previous studies have been on double-arm spiral antennas, because they have lower structural complexity than multi-arm ones (in fact, always four-arm). However, with the development of satellite communications, the multi-mode excitation capability of the four-arm spiral antenna makes it widely applied to monopulse direction finding systems [3]. Moreover, for high-precision GNSS, the highly symmetrical structure of the four-arm spiral antenna enables better phase stability [4].

The difficulty in the spiral antenna design is the broadband impedance matching. Because the inherent impedance of the spiral antenna is greater than 90Ω, an impedance transformer is required between the spiral antenna and the 50Ω input port. For two-arm spiral antennas, they are often fed by infinite baluns [5], vertical to parallel coaxial baluns [6] and the latest improved Dyson-style baluns [7], [8] in recent years. In order to solve the matching problem of the four-arm spiral antenna, the impedance should be reduced to about 50Ω, available methods are as followed: feeding the spiral hole by a four-port coaxial beam, modifying the metal groove ratio of the spiral hole [9], using double-layer spiral and thicker dielectric substrate [10].

The associate editor coordinating the review of this manuscript and approving it for publication was Chinmoy Saha.

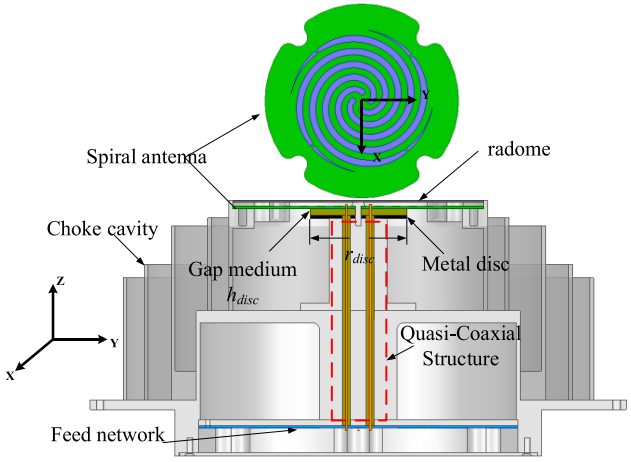

FIGURE 1. Geometry of the proposed antenna.

Influenced by multipath and surface waves, many antennas have an unstable phase center which is very important for wide-beam antenna design. To deal with it, the choke is often applied in antennas. A typical choke consists of equal deep concentric rings on a circular metal ground plane [13], [14]. In [16], a new type of broadband ground plane that works in a broadband 1.15-1.6 GHz is presented. Its height is shallower than that of a choke and its volume is 40% smaller than that of an equivalent choke antenna. In [17], an antenna with better multipath suppression and a smaller size is realized, by adopting a sawtooth structure and a vertical small choke at the bottom. However, these designs require more complicated corrugated rings, which increase the complexity and are difficult to manufacture.

This letter proposes a novel quasi-coaxial-fed four-arm planar spiral antenna, which is suitable for GNSS application. The impedance transformation is completed by loading a coupling metal disc and a new type quasi-coaxial structure as the balun. A broadband network with stable amplitude and phase difference is provided to obtain a good broadband circular polarization performance. What's more, the chokes of uneven depths are located around the antenna, therefore a stable phase center and high front-to-back ratio can be achieved. Through verification, the proposed antenna exhibits good matching and radiation characteristics in 1.1-1.7 GHz, and the simulation and measured results agree well, verifying the feasibility of the design.

II. DESIGN OF THE ANTENNA

As shown in Fig. 1, the novel spiral is composed of four parts: a spiral antenna and a feed network are placed separately on the top and bottom, feed structure with a metal disc and four quasi-coaxial lines is fixed in the middle of the chokes, and chokes with uneven depths on both sides. A printed circuit board (PCB) is placed on the metal disc, separated by a media of the same size as the disc. The feed network connected to four quasi-coaxial lines is at the back of the choke. Detailed discussion is as follows.

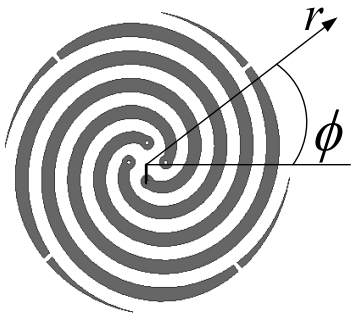

FIGURE 2. Geometry of the Archimedean spiral.

A. FOUR-ARM SPIRAL

This article uses a four-arm planar Archimedes spiral antenna, and its structure is shown in Fig. 2. The equation for the inner and outer edge lines of one of the spiral arms is:

$$r_1 = a(\phi - \delta/2) + r_0 \tag{1}$$

$$r_2 = a(\phi + \delta/2) + r_0 \tag{2}$$

where r_0 is spiral starting radius (mm), α is growth rate (mm/rad), and ϕ is azimuth (rad). For a perfectly self-complementary structure, the width of the gap between two adjacent arms is equal to the width of the spiral arm, that is, $\delta = 45°$. The remaining arms are formed by rotating 90°, 180°, and 270° around the axis perpendicular to the spiral plane.

The impedance of an N-arm self-complementary spiral antenna to the ground can be obtained as follows [22]:

$$Z_{free} = \frac{\eta_0/4}{\sin(\pi/N)} \tag{3}$$

where η_0 is the free space wave impedance of 120π. In practice, the spiral antenna is printed on a dielectric substrate with $\varepsilon_r = 4$. The half-space impedance can be approximated as Z_{free}/sqrt (ε_{eff}), where ε_{eff} is the effective permittivity of the dielectric substrate, usually $(\varepsilon_r + 1)/2$. Therefore, the actual impedance of the antenna is usually less than the theoretical value [23] about 100Ω, as shown in Fig. 3.

The radiation characteristic of the antenna is determined by its distributed current. As Fig. 4 depicts, the current on the proposed four-arm spiral antenna gradually attenuates from the center to the end. But due to the truncation effect, there is still a small amount of current at the end of the spiral, which will deteriorate the radiation characteristics of the antenna. Usually, an end loading can be used to reduce the negative impact of reflected current. However, no matter loading resistance or absorbing material, they both pose a risk of radiation efficiency decrease. In this paper, the tapered end loading is adopted to improve the radiation performance.

B. CONFIGURATION OF FEED

From the analysis above, it can be known that the impedance of the four-arm spiral antenna with self-complement structure is about 100 Ω, which is difficult to match with the feeding

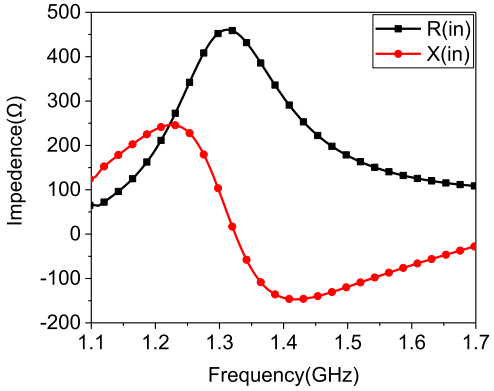

FIGURE 3. The impedance of the four-arm spiral antenna.

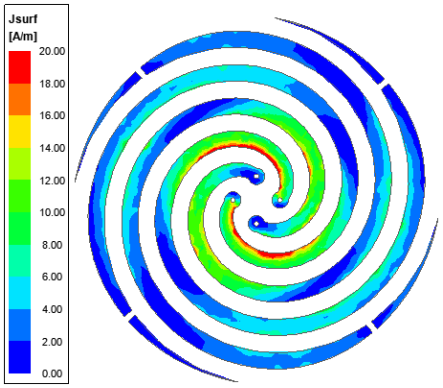

FIGURE 4. The current on the four-arm spiral at 1.4GHz.

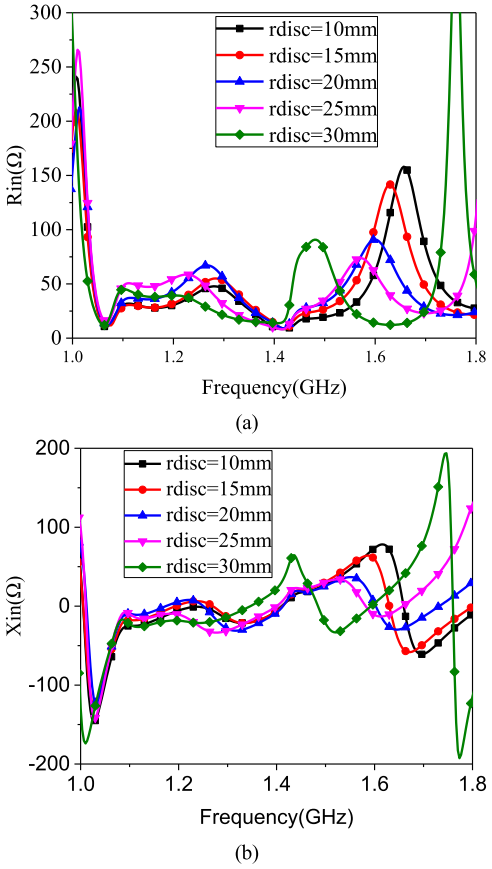

FIGURE 5. Simulated impedance for the proposed antenna as the r_{disc} changed.

network. In order to solve this problem, we designed a new feed structure, and antenna is excited using four quasi-coaxial lines which consist of a copper rod core and a hollow dielectric medium. A metal disc used as an induction capacitor is loaded to adjust the input impedance of the antenna. The distance between the spiral arm plane and the disc is represented as parameter h_{disc}. The radius of the disc is the parameter r_{disc}. Perform simulation researches by changing the geometric parameters to observe the changes on the impedance performance of the antenna. Unless specially indicated, only one geometrical parameter is varied each time and the rest is kept unchanged.

1) EFFECTS OF RADIUS OF THE DISC

Fig. 5 shows the real and imaginary parts of the input impedance when only the disc radius $r_{disc} = 10$ mm, 15 mm, 20 mm, 25 mm, and 30 mm are changed, and the parameter disc spacing $h_{disc} = 3$ mm remains unchanged. The smoother the antenna impedance curve, the better its frequency characteristics. In order to provide a better match for the subsequent network and antenna overall structure design, we choose $r_{disc} = 25$mm. Because the real part of the impedance is about 50Ω in the 1.1-1.7GHz bandwidth, the imaginary part of the impedance tends to 0Ω, and the curve is relatively flat.

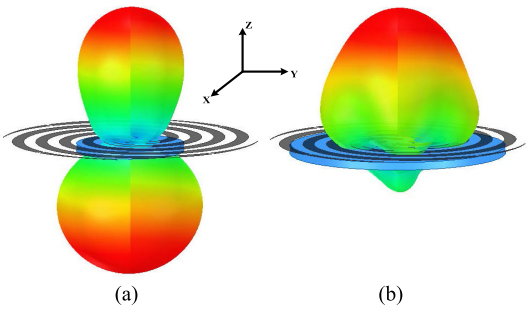

FIGURE 6. Simulated and measured (a) r_{disc}, = 10mm (b) r_{disc} = 40 mm.

According to the current band theory (CB theory) [15], the main active area responsible for radiation is an annular area whose perimeter on the spiral plane corresponds to a wavelength at the operating frequency f, that is, $2\pi r = 2\pi r f_{irst} = \lambda_f$. When the radius of the main active area at the corresponding frequency point is greater than r_{disc}, the disk does not function as a reflector, so it produces bidirectional radiation in the positive and negative Z directions, as shown in Fig. 6 (a). On the contrary, as the frequency increases, the radius becomes smaller than the radius of the disc (i.e., $r_{first} < r_{disc}$), the disc acts as a reflector. As shown in Fig. 6 (b), the antenna has positive Z directional radiation.

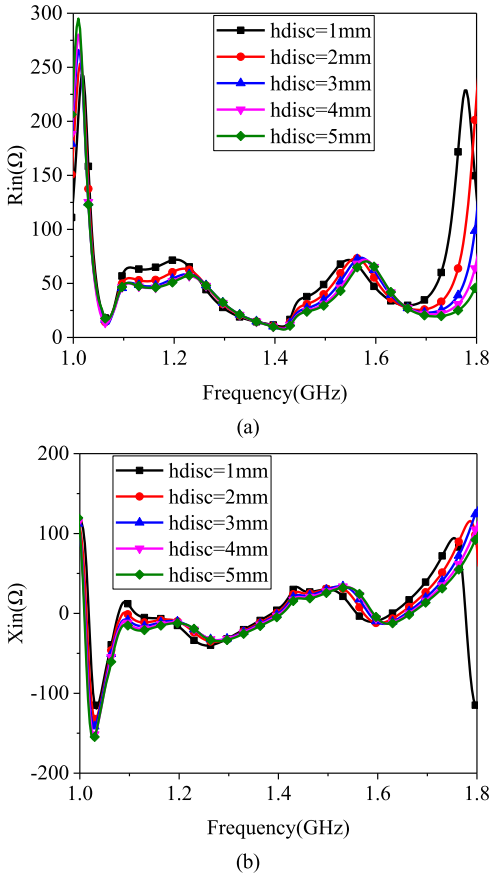

FIGURE 7. Simulated impedance for the proposed antenna as the h_{disc} changed.

2) EFFECTS OF DISTANCE BETWEEN THE DISC AND ANTENNA

The effect of the distance h_{disc} (between the spiral arm plane and the disc), on the impedance performance is shown in Fig.7 where h_{disc} changing from 1 mm to 5 mm. As it depicts, the real and imaginary parts of the antenna input impedance hardly change, when the radius of the disc is constant.

C. DESIGN OF CHOKE

Most multipath signals in the environment arrive from below the antenna or low elevation angles. Therefore, the antenna is designed with a sharply reduced pattern, that is, low back lobe and low sidelobe to suppress multipath signals [16]. And to prevent the surface wave generated by the multipath signal from affecting the antenna performance [17], the choke ground plane is usually used with the reference antenna. It is necessary to suppress surface waves near the antenna, so a choke is used together with the antenna.

As shown in Fig. 8, conventional choke is a corrugated metal structure composed of several concentric metal rings of equal height on a metal base. Changes in the structure of the choke will affect two types of surface waves: transverse electric (TE) and transverse magnetic (TM) surface waves. On the one hand, TE surface wave requires surface impedance to be capacitive. On the other hand, TM surface wave requires

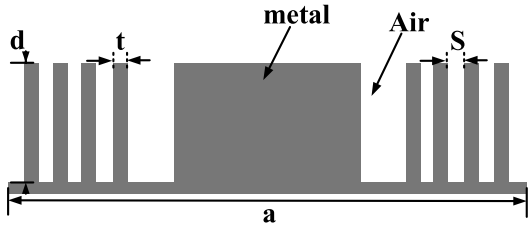

FIGURE 8. Cross-sectional view of a conventional equal-depth metallic choke with dimensions a = 380 mm, d = 63 mm, s = 25 mm, and t = 3 mm [24].

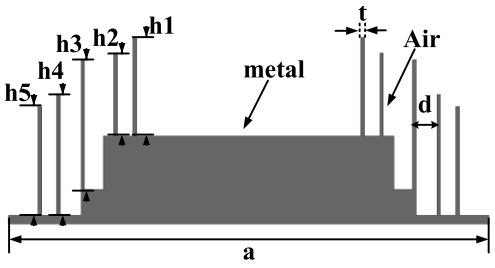

FIGURE 9. Cross-sectional view of a new type unequal-depth metallic choke.

surface impedance to be inductive [15]. The suppression of TE surface wave is to use the metal surface of the choke [18]. However, the corrugation depth of the choke controls the TM surface wave. The surface impedance of the choke is calculated by analogy with the input impedance of a short-circuit transmission line [18]

$$Z_s = jZ_0 \tan kd \tag{4}$$

In (4), $Z_0 = 377\ \Omega$ is the inherent impedance of air or free space, d is the ripple depth, and k is the phase constant.

Next, analyzing the influence of the choke on the propagation of TM surface waves under different corrugation depths. When the corrugation depth is $0 \leq d \leq \lambda/4$, the surface impedance is inductive, and it supports the propagation of TM surface waves. But when the corrugation depth is $\lambda/4 \leq d \leq \lambda/2$, the surface impedance is capacitive, so this is the characteristic of suppressing TM surface wave required in the choke, and as the depth d is closer to $\lambda/4$, TM The suppression of surface waves is stronger [15]. Based on the above analysis, it is recommended to use a corrugated structure with a depth of $\lambda/4$ to suppress multipath signals.

For broadband antennas, different operating frequencies correspond to different wavelengths. If the same ripple depth is used, it can only suppress surface waves near the corresponding frequency point. Therefore, different ripple depths are required to suppress TM surface waves of different frequencies. As shown in Fig. 9, a new type of choke is designed. Its corrugation depth is different, which has a good suppression effect on different working frequencies. The final parameters after optimization are shown in Table 1. In order to verify the suppression effect of the uneven-depth chokes we designed, the GNSS antenna is simulated with full-wave simulation in the three cases without choke, traditional choke

TABLE 1. Parameters of the designed choke.

h1	h2	h3	h4	h5	t	d	a
57mm	48mm	75mm	70mm	63mm	2mm	12mm	278mm

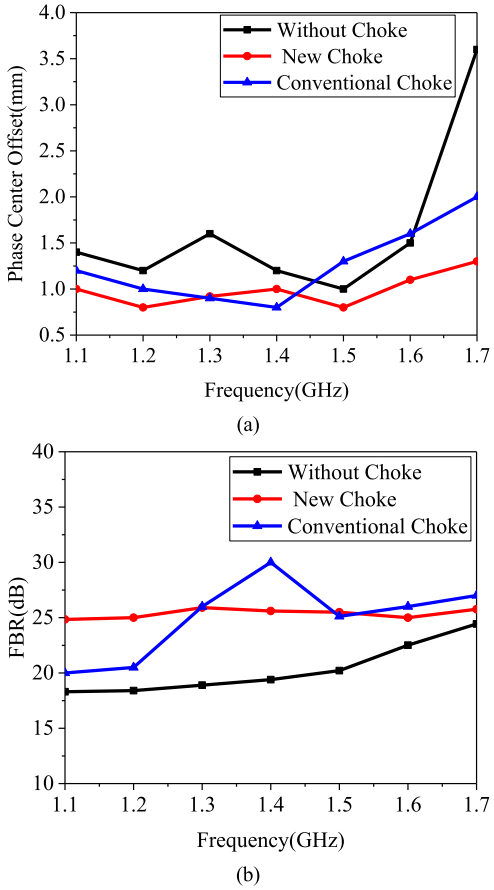

FIGURE 10. (a) Phase center stability and (b) Front-to-back ratio comparison at different choke types.

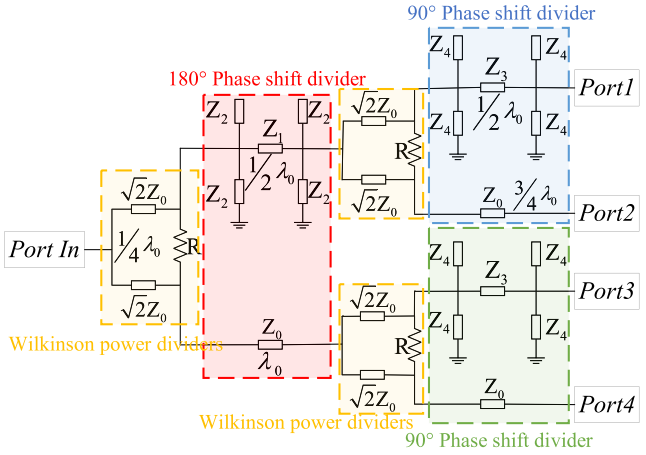

FIGURE 11. Schematic of the proposed feed network.

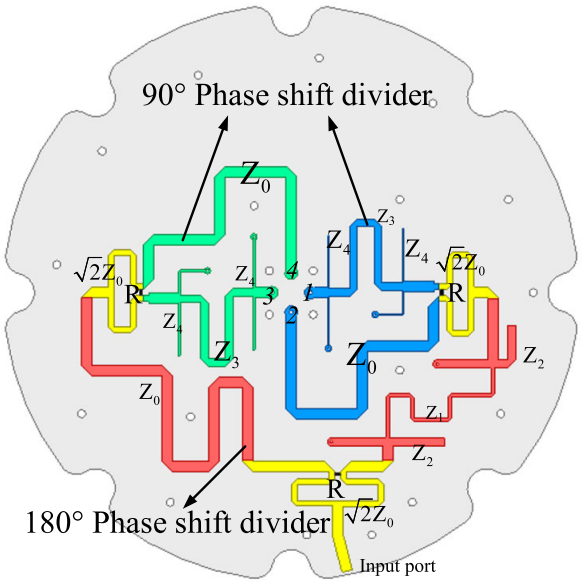

FIGURE 12. Photo of the proposed feed network.

(corrugation depth is λ/4), and new choke. The calculation results are shown in Fig.10.

As shown in the figure, the new-type choke slot antenna has good phase center stability (less than 1.5mm) and front-to-back ratio (greater than 25dB) in the 1.1-1.7GHz frequency band; The traditional choke slot has a good suppression effect at the center frequency point. When the frequency changes, the effect starts to deteriorate. The antenna phase center stability and front-to-back ratio deteriorate without choke slot. The simulation results are consistent with the theory.

D. FEED NETWORK CONFIGURATION

The input current of the adjacent arms of the multi-arm helical antenna should satisfy the same amplitude and phase difference of 90° in sequence, with good CP performance and stable phase center [20]. The performance of the feed network, especially the stability of the amplitude difference and the phase difference, has a huge impact on the performance of the final antenna. The 90° phase shift bandwidth of the traditional λ/4 phase shifter is extremely narrow and cannot be matched to a broadband antenna. In order to feed the proposed antenna, a broadband feed network consisted of three Wilkinson power dividers and three broadband phase shifters was designed [21]. The network includes a 180° phase shift divider and two 90° phase shift dividers. The specific characteristic impedance of each section of the transmission line of the designed feeder network is shown in Fig. 11. Fig. 12 is a schematic diagram of the distribution of network transmission lines.

According to [9], when the characteristic impedance of the port Z0 = 50 Ω, to achieve a broadband 90° phase shift requires: Z1 = 61.9 Ω, Z2 = 125.6 Ω; the conditions for achieving a 180° phase shift are Z3 = 80.8 Ω, Z4 = 62.8 Ω. Then, by appropriately adjusting the width of each microstrip line, a broadband feeder network with a center frequency of 1.4 GHz is realized. Fig. 13 (a) and (b) show the analog amplitude response and phase shift of each output port in the 1.1-1.7 GHz band. The designed network has excellent

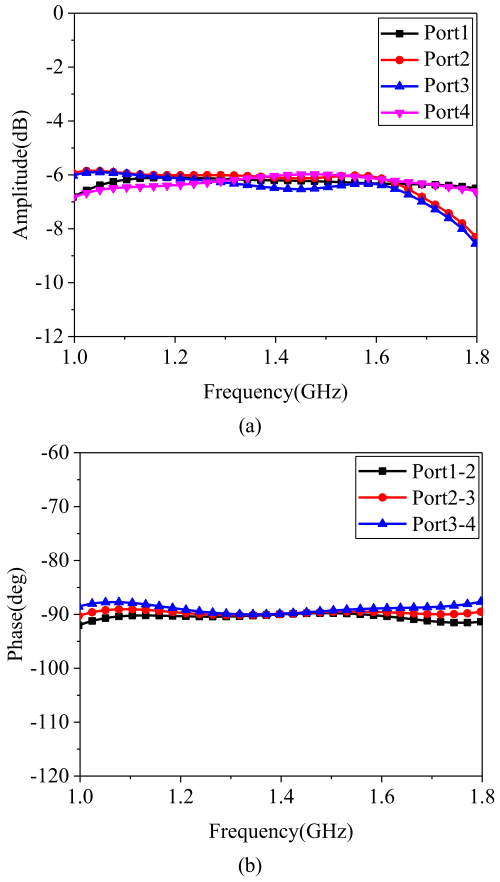

FIGURE 13. Simulated (a) magnitude response and (b) phase difference of the proposed feed network.

performance, the amplitude change is less than 0.5 dB, and the phase shift unbalance is less than 3°.

III. FABRICATED ANTENNA AND MEASUREMENTS

A. CONFIGURATION OF THE ANTENNA

According to the above simulation design and numerical analysis results, the main parameters of the proposed antenna are as follows:

B. PERFORMANCE OF THE ANTENNA

The simulation design of the antenna is done using full-wave simulation. All microstrip lines of the antenna are silver-plated to prevent oxidation. Fig. 15 shows the simulation and measurement results of the antenna. A vector network analyzer is used to measure the voltage standing wave ratio (VSWR) which is less than 1.5 in the entire 1.1-1.7GHz bandwidth. The radiation character is measured in the anechoic chamber. The measured 3-dB AR bandwidth exceeds 0.6 GHz (1.1 GHz-1.7 GHz), which can cover the entire GNSS frequency band, and the gain exceeds 7.4dBic. In addition, the designed antenna phase center is stable, and the change is less than 1.5mm in the required frequency band [11]. The actual processing and testing performance of the antenna is good.

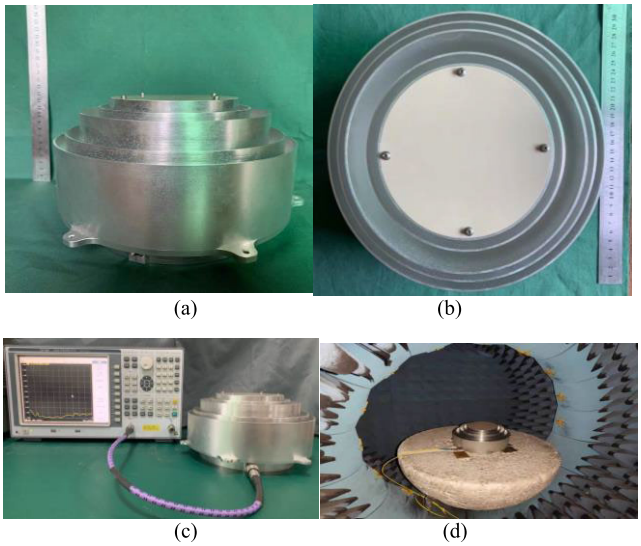

FIGURE 14. Photographs of and test setup for the fabricated antenna: (a) front view, (b) top view, (c) vector network analyzer test, and (d) anechoic chamber test.

TABLE 2. Parameters of the designed antenna.

Dielectric substrate of radome, ε_1	3.3
Substrate thickness of radome, h_1	1mm
Dielectric substrate of spiral, ε_2	4.1
Substrate thickness of spiral, h_2	1.5mm
Radius of the disc, r_{disc}	25mm
Width/gap of the spiral and disc, h_{disc}	3mm
Number of turns for spiral	1.25
Overall radius of the antenna, r	115mm
Start radius of the antenna, r_{in}	4mm
Growth rate of the spiral, α	5.6
Dielectric substrate of feed network, ε_3	3.55
Substrate thickness of feed network, h_3	1.524mm

Processing errors are inevitable in the antenna manufacturing process, so there is a slight deviation between the simulation and measurement results. In addition, the antennas we proposed are used in GNSS, so we focus on giving the simulated and measured radiation patterns at frequencies of 1149, 1176, 1227, 1268, 1575, and 1593MHz. Due to the choke and the disc, the antenna only radiates to the +Z axis in one direction, and the cross polarization is suppressed to the level of −20dB. More importantly, the antenna radiation pattern has a wide beam characteristic, as shown in Fig. 16, the gain is greater than 0 dBic in the range of −60° to 60°.

C. COMPARISON

Table 3 lists the key performance comparisons between the proposed antenna and other similar broadband GNSS antennas. It can be seen that the antenna proposed by

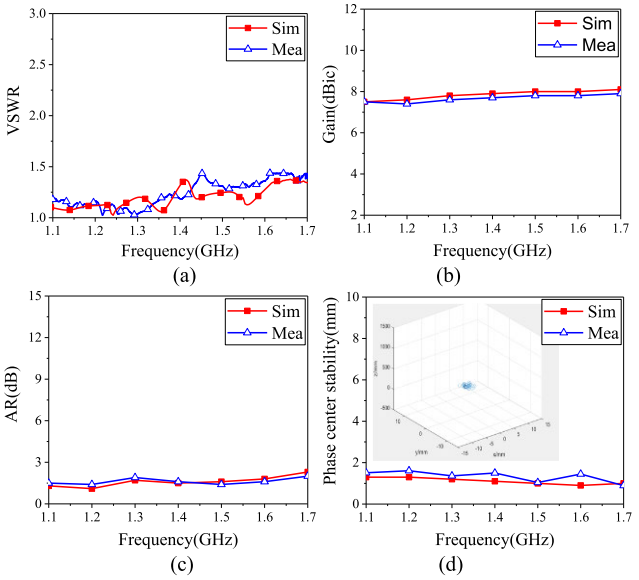

FIGURE 15. Simulated and measured (a) return loss, (b) gain, (c) axial ratio, and (d) phase center stability of the proposed antenna.

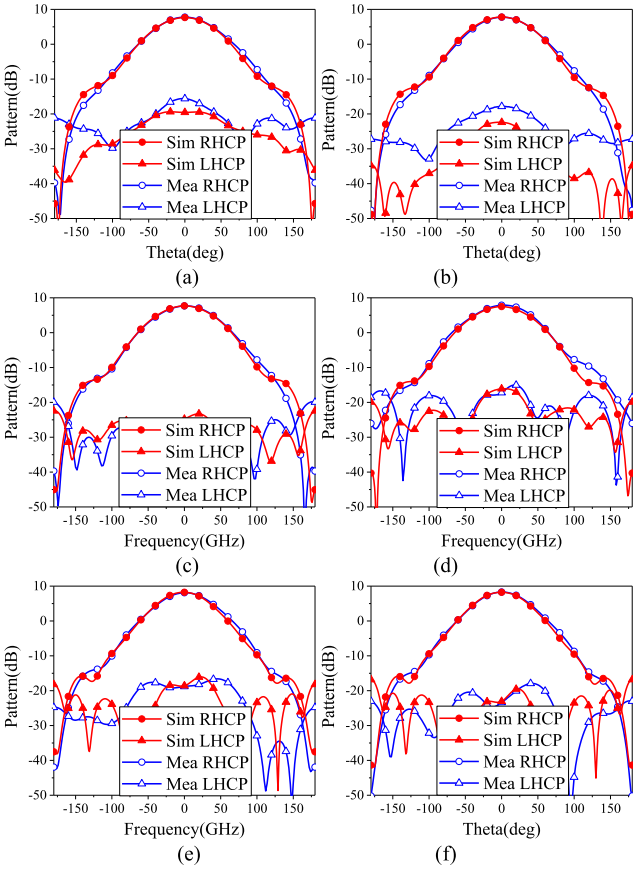

FIGURE 16. Measured CP radiation pattern of the proposed antenna at the frequency of (a) 1149, (b) 1176, (c) 1227, (d) 1268, (e) 1575 and (f) 1593 MHz.

comprehensive broadband, dimensions, gain, high front-to-back ratio and phase center stability and other indicators has good performance. Moreover, compared with other spiral antennas, the designed antenna has a simple and effective impedance matching adjustment device. Therefore, considering all the indicators, this antenna has excellent performance and is very suitable for GNSS system.

TABLE 3. Comparison of wideband GNSS antennas.

Ref.	-10-dB IBW (%, GHz)	Dimensions (λ_0)	Gain (dBic)	FBR (dB)	PCD (mm)	3dB AR beamwidth
[10]	9.24 (1.52-1.67)	0.43×0.43×0.03	3.2	15	1.19	124°
[12]	25.4 (1.44-1.86)	0.37×0.48×0.01	1.3	22	8.8	60°
[17]	31.7 (1.17-1.61)	0.71×0.71×0.46	7.0	25	--	70°
[18]	32.7 (1.15-1.60)	1.56×1.56×0.28	6.0	20	3.0	--
[19]	2.0 (1.55-1.59)	1.57×1.57×0.05	4.5	28	2.5	75°
[20]	31.9 (1.16-1.61)	0.77×0.77×0.55	7.5	25	--	--
This work	43.8 (1.1-1.7)	1.14×1.14×0.62	7.4	25	1.5	116°

IV. CONCLUSION

In this letter, a novel type of quasi-coaxial-fed four-arm planar spiral antenna is proposed. This design realizes the necessary impedance transformation between the high impedance of the spiral aperture and the input impedance of 50Ω by introducing a metal disc and a quasi-coaxial structure. Broadband feed networks and chokes improve the right-hand circular polarization (RHCP) radiation performance. Simulation and actual measurement results show that the proposed antenna has good matching and radiation characteristics. The low angle (elevation angle = ±60°) gain is above 0dBic, the axial ratio is less than 3dB, and the phase center change is less than 1.5mm over the whole GNSS bands. In addition, low profile and firmness make the antenna have broad application prospects in GNSS system.

REFERENCES

[1] B. A. Kramer, S. Koulouridis, C. C. Chen, and J. L. Volakis, "A novel reflective surface for an UHF spiral antenna," *IEEE Antennas Wireless Propag. Lett.*, vol. 5, pp. 32–34, 2006.

[2] A. A. Heidari, M. Heyrani, andM. Nakhkash, "A dual-band circularly polarized stub loaded microstrip patch antenna for GPS applications," *Prog. Electromagn. Res.*, vol. 92, pp. 159–208, 2009.

[3] C. M. Su and K. L. Wong, "A dual-band GPS microstrip antenna," *Microw. Opt. Techn. Lett.*, vol. 33, no. 4, pp. 238–240, May 2002.

[4] L. Boccia, G. Amendola, and G. D. Massa, "A dual frequency microstrip patch antenna for high-precision GPS applications," *IEEE Antennas Wireless Propag. Lett.*, vol. 3, pp. 157–160, 2004.

[5] G. A. E. Vandenbosch and A. R. Van de Capelle, "Study of the capacitively fed microstrip antenna element," *IEEE Trans. Antennas Propag.*, vol. 42, no. 12, pp. 1648–1652, Dec. 1994.

[6] P. C. Werntz and W. L. Stutzman, "Design, analysis and construction of an Archimedean spiral antenna and feed structure," in *Proc. IEEE Energy Inf. Technol. Southeast*, vol. 1, Apr. 1989, pp. 308–313.

[7] T.-K. Chen and G. H. Huff, "Stripline-fed Archimedean spiral antenna," *IEEE Antennas Wireless Propag. Lett.*, vol. 10, pp. 246–249, 2011.

[8] S. Kim, M. M. Tentzeris, G. Jin, and S. Nikolaou, "Inkjet printed ultra wideband spiral antenna using integrated balun on liquid crystal polymer (LCP)," in *Proc. IEEE Int. Symp. Antennas Propag.*, Jul. 2012, pp. 1–2.

[9] D. S. Filipovic, A. U. Bhobe, and T. P. Cencich, "Low-profile broadband dual-mode four-arm slot spiral antenna with dual Dyson balun feed," *IEE Proc., Microw., Antennas Propag.*, vol. 152, pp. 527–533, Dec. 2005.
[10] K.-K. Zheng and Q.-X. Chu, "A novel annular slotted center-fed BeiDou antenna with a stable phase center," *IEEE Antennas Wireless Propag. Lett.*, vol. 17, no. 3, pp. 364–367, Mar. 2018.
[11] A. Kumar, A. D. Sarma, E. Ansari, and K. Yedukondalu, "Improved phase center estimation for GNSS patch antenna," *IEEE Trans. Antennas Propag.*, vol. 61, no. 4, pp. 1909–1915, Apr. 2013.
[12] Y. Cao, S. W. Cheung, and T. I. Yuk, "A simple planar polarization reconfigurable monopole antenna for GNSS/PCS," *IEEE Trans. Antennas Propag.*, vol. 63, no. 2, pp. 500–507, Feb. 2015.
[13] D. J. Sawyer, S. Das, N. Diamanti, A. P. Annan, and A. K. Iyer, "Choke rings for pattern shaping of a GPR dipole antenna," *IEEE Trans. Antennas Propag.*, vol. 66, no. 12, pp. 62–65, Dec. 2018.
[14] D. Li, L. Li, Z. Li, and G. Ou, "Four-arm spiral antenna fed by tapered transmission line," *IEEE Antennas Wireless Propag. Lett.*, vol. 16, pp. 2008–2011, 2017.
[15] R. E. Collin, *Field Theory of Guided Waves*, 1st ed. New York, NY, USA: McGraw-Hill, 1960.
[16] M. K. Emara, J. Hautcoeur, G. Panther, J. S. Wight, and S. Gupta, "Surface impedance engineered low-profile dual-band grooved-dielectric choke ring for GNSS applications," *IEEE Trans. Antennas Propag.*, vol. 67, no. 3, pp. 2008–2011, Mar. 2019.
[17] S. Liu, D. Li, B. Li, and F. Wang, "A compact high-precision GNSS antenna with a miniaturized choke ring," *IEEE Antennas Wireless Propag. Lett.*, vol. 16, pp. 2465–2468, 2017.
[18] F. Scire-Scappuzzo and S. N. Makarov, "A low-multipath wideband GPS antenna with cutoff or non-cutoff corrugated ground plane," *IEEE Trans. Antennas Propag.*, vol. 57, no. 1, pp. 33–46, Jan. 2009.
[19] R. Baggen, M. Martinez-Vazquez, J. Leiss, S. Holzwarth, L. S. Drioli, and P. de Maagt, "Low profile GALILEO antenna using EBG technology," *IEEE Trans. Antennas Propag.*, vol. 56, no. 3, pp. 667–674, Mar. 2008.
[20] R. H. Johnston, "Development of a high performance GNSS antenna," in *Proc. IEEE Antennas Propag. Soc. Int. Symp. (APSURSI)*, Memphis, TN, USA, Jul. 2014, pp. 1654–1655.
[21] X. Ren, S. Liao, and Q. Xue, "A circularly polarized spaceborne antenna with shaped beam for earth coverage applications," *IEEE Trans. Antennas Propag.*, vol. 67, no. 4, pp. 2235–2242, Apr. 2019.
[22] G. Deschamps, "Impedance properties of complementary multiterminal planar structures," *IRE Trans. Antennas Propag.*, vol. 7, no. 5, pp. 371–378, Dec. 1959.
[23] M. McFadden and W. R. Scott, Jr., "Analysis of the equiangular spiral antenna on a dielectric substrate," *IEEE Trans. Antennas Propag.*, vol. 55, no. 11, pp. 3163–3171, Nov. 2007.
[24] M. K. Emara, K. Madhoun, R. Madhoun, and S. Gupta, "A low-cost light-weight 3D-printed choke ring for multipath mitigation for GNSS antennas," in *Proc. IEEE Int. Symp. Antennas Propag. USNC-URSI Radio Sci. Meeting*, Jul. 2019, pp. 721–722, doi: 10.1109/APUSNCURSINRSM.2019.8888998.

LILI GUO was born in Gansu, China. She received the bachelor's degree from Xidian University, Xi'an, China, in 2019, where she is currently pursuing the M.Eng. degree. Her current research interest includes broadband array antennas.

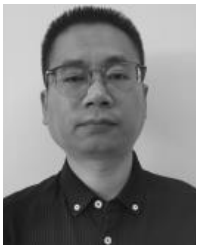

PEIHUA ZHANG was born in China, in 1981. He received the bachelor's degree from the School of Mathematics, Sichuan University, in 2005. He joined The 20th Research Institute of China Electronics Technology Corporation, in 2005, and currently works as a Senior Engineer. He has published dozens of articles, many of which have been indexed by SCI and EI. His main research interests include satellite navigation, area navigation, and low-orbit navigation.

FANCHAO ZENG was born in Shandong, China, in 1995. He received the bachelor's and master's degrees in electronic and information engineering from Xidian University, Xi'an, China, in 2018 and 2021, respectively. He is currently pursuing the Ph.D. degree with the University of Technology Sydney (UTS), Australia.

His current research interests include dielectric resonator antennas, spiral antennas, and array antennas.

ZHIYA ZHANG was born in Yancheng, China, in 1985. He received the Ph.D. degree from Xidian University, Xi'an, China, in 2012.

He is currently an Associate Professor with the National Key Laboratory of Antennas and Microwave Technology, Xidian University. His current research interests include broadband antennas, millimeter-wave antennas, and antenna arrays.

CHENGBIN ZHANG was born in Lanzhou, China, in 1981. He received the bachelor's and master's degrees from Xidian University, where he is currently pursuing the Ph.D. degree. His research interests include microstrip antennas and slot antennas.